# INNOVATIVE RESTRAINTS TO PREVENT CHEST INJURIES IN FRONTAL IMPACTS

**Francisco J. Lopez-Valdes**
**Oscar Juste-Lorente**
Institute of Engineering Research (I3A), University of Zaragoza
Spain

Paper Number 15-0381

## ABSTRACT

By 2050, 21% of world population is expected to be older than 60 years. This age shift poses a serious challenge to the protection of car occupants, as fragility and frailty are associated to increasing age. Advanced restraint systems that aim to reduce chest loading by implementing load limiters or inflatable parts have been introduced in the market over the last years. This paper investigates the kinematics and dynamics of two surrogates (THOR dummy, Post Mortem Human Surrogates or PMHS) in 35 km/h impacts under the action of two different restraints: a pretensioning, force-limiting seat belt (PT+FL) and a concept design consisting of two separate shoulder and lap belt bands (split buckle system or SB). Three repeats per condition where done with the THOR dummy, while only one PMHS was tested per restraint system. With respect to the PT+FL, the results from the THOR tests showed that the SB seat belt decreased chest deflection significantly without a substantial increase of the forward displacement of the head. The PT+FL belt allowed the pelvis of the PMHS to move forward preventing the rotation of the torso and therefore reducing the forward excursion of the head. The PMHS test with the SB resulted in improved kinematics compared with the PT+FL. A complete understanding of the kinematics and dynamics induced by these restraints would require additional PMHS tests.

## INTRODUCTION

Life expectancy in Europe rose by eight years between 1960 and 2006 [1]. Additionally, the number of births has declined continuously over the last decades, resulting in an increase of the proportion of elderly people in the European population. While in 2012 about 17% of all Europeans were aged 65 and older, the share of those over age 65 will rise to 28% in 2020 [2]. According to United Nations, the same trend is observed in the whole world although it is particularly important in Eastern Asia (Japan, China, Mongolia), Europe and North America. Interestingly, fast population ageing will take place mainly in the less developed regions. Globally, it is forecasted that world's population age 60 years or over will increase over the following years to reach 21% in 2050 [3].

In 2010, 6,563 elderly people were killed in road traffic accidents in the 24 European Member States for which CARE data is available [4]. This constitutes 21.7% of fatalities of all ages in 2010. What is even more significant is that the the proportion of elderly fatalities has been increasing steadily for the last 10 years. While this increase is undoubtely related to a higher exposure of this age group, it is also true that increased frailty and fragility are associated to aging. Contemporary research has shown that should the injury risk of the elderly was similar to that of a 20-year-old car occupant, some 10,000 lives could be saved in the United States [5]. Therefore, given the existing trend of a growing proportion of elderly road users, it is mandatory to recognize their physiological differences and to incorporate their peculiarities into the design of more effective restraints. A review of AIS3+ injuries within NASS CDS shows that as age increases from 15 to 75+ years old, the incidence of thoracic injuries increases and becomes the most frequent serious injury among car occupants older than 46 years old, and accounting for more than 35% of all AIS3+ injuries in people aged 75 years and above [6]

Force-limiting seatbelts in combination with airbags have been shown to reduce significantly chest loading and consequently chest injuries, without increasing the risk of a head impact [7,8]. The combination of pretensioners and force limiters in rear seat restraints has been also shown to allow greater torso rotation of the occupant without increasing significantly the peak forward excursion of the head and therefore without increasing the risk of head contact [9,10]. In recent years, inflatable seatbelts have been discussed as a countermeasure that can reduce the risk of chest injuries even further by increasing the area of the torso on which the seatbelt force is applied and incorporating a damping effect in addition to the elastic component of conventional belt webbing [11-14]. These innovative restraints have been shown to modify substantially the kinematics of the occupants, challenging existing knowledge about the

optimal seatbelt geometry and position of belt anchorages [14]. With the continuous improvement of finite element human body models (HBM), parametric analyses constitute an effective methodology to optimize the design of innovative restraint systems. Real testing with Anthropomorphic Test Devices (ATD) also allows to confirm that existing testing tools are sensitive to newly designed restraint systems. However, it is also necessary that both surrogates (HBM and ATD) are able to capture the effects of these restraints on real human subjects. Thus, Post Mortem Human Surrogate (PMHS) testing is advisable to acquire a more accurate picture of the potential benefit that these system can bring to elderly car occupants.

The present study discusses the performance of the THOR ATD and the mechanical response of two PMHS exposed to a frontal impact and restrained by two different seatbelt solutions. The kinematics and dynamics of both surrogates will be compared with the goal of assessing if a new seatbelt concept is capable of reducing chest deflection without increasing other important performance indices.

## METHODS

Eight sled tests in matching conditions were performed at the crash test facility of the Institute of Enginering Research (I3A) of the University of Zaragoza. Two Post Mortem Human Surrogates (PMHS) were exposed to a 35 km/h (nominally) frontal impact, using two different restraints. Then, the THOR dummy was exposed to nominally the same test conditions and using the same two types of restraints than in the PMHS tests. Three repeats were done per restraint type with the THOR dummy. The test matrix is shown in Table 1. The time history of sled deceleration is included in Figure A1 and Figure A2 in the Appendix.

**Table1.**
**Test matrix.**

| Occupant type | # runs | Restraint | Impact speed (km/h) |
|---|---|---|---|
| PMHS | 1 | SB | 37.7 |
| PMHS | 1 | PT+FL | 34.6 |
| THOR | 3 | SB | 34.8±0.2 |
| THOR | 3 | PT+FL | 34.7±0.0 |

### Test setup

The test fixture consisted of a rigid metallic frame allowing complete visual access to the occupant while preserving the basic geometry of a standard seating position of a passenger car. This test fixture has been used elsewhere as a reasonable approximation to the passenger posture in the study of ATD biofidelity and in the development of thoracic injury criteria [15,16]. The seat consisted of a flat steel plate with two pelvic supports at the rear. Forward motion of the occupant was restrained by two different seat belts: a retractor pretensioned (2 kN), force-limiting (4 kN) belt (PT+FL) and an innovative belt consisting on two independent shoulder and lap bands (SB). The SB shoulder belt band was retractor pretensioned (3 kN) and the lap belt band was pretensioned at 3.5 kN bilaterally. The position of the buckle of the lower shoulder belt band was forward of that of the inner buckle of the lap belt with the goal of unloading the lower part of the rib cage. As for the position of the D-ring, it was modified accordingly to the specific dimensions and anthropometry of the different surrogates to ensure that the upper shoulder belt angle measured between the shoulder of the occupant and the D-ring was the same. Belt tension was measured at several locations both on the shoulder and on the lap seat belts for each system. Sensor data in the ATD and PMHS tests were captured at 10,000 Hz with an external data acquisition system (PCI-6254, National Instruments; Austin, TX). The kinematics of the surrogates were recorded by a lateral and a frontal high-speed imager at 1,000 Hz.

### THOR tests

The THOR ATD used in this study is the THOR-NT upgraded within the THORAX project (European 7th Framework Program) to improve biofidelity and injury assessment capabilities [17,18]. This THORAX THOR (further denoted as simply THOR) is similar to the U.S version THOR Mod Kit with SD3 shoulder.

ATD head was instrumented with a 6-degree-of-freedom (DOF) cube including three linear accelerometers and three angular rate sensors (ARS) oriented in perpendicular directions acoording to SAE J211 recommendations. Two 6-axis load cells were present at the upper and lower neck locations. Chest instrumentation included four 3D IR-TRACCs (Infra-Red Telescoping Rod for the Assessment of Chest Compression) and 72 strain gauges distributed from rib 2 to rib 7 bilaterally (equally spaced along the rib). The dummy was equipped with a 96-channel digital on-board data acquisition system to supplement the external one.

A high-speed motion capture system consisting of 10 cameras was used to track the position of retroreflective spherical markers within a calibrated 3D volumen at 1,000 Hz (Vicon, TS series, Oxford, UK). A calibration procedure, performed prior to testing, established the position and orientation of each camera in a reference coordinate system at a laboratory fix location. A local coordinate system moving with the test buck was defined so that the relative motion between the occupant and the buck could be resolved. The local X axis pointed forward in the direction of the sled motion and the local Z axis pointed upwards. Displacements were calculated with respect to the local coordinate system. Reflective markers were attached to several relevant anatomical locations in the dummy, although only the head ones (attached bilaterally and over the line passing through the center of gravity of the head) were used in this study.

**PMHS tests**

The two PMHS tests used in this study as comparison with the THOR dummy were carried out within the 7th Framework Program Marie Curie Action BIO-ADVANCE [19]. The procurement and handling of PMHS were done according to the internal procedures of the laboratory of the I3A (University of Zaragoza). These procedures were reviewed and approved by the laboratory Oversight Committee and by the Ethical Commission for Clinical Trials of Aragon (CEICA), which is the officially appointed regional committee that supervises the ethics of all clinical trials performed within the region. CEICA is totally independent from the University of Zaragoza and reports directly to the Health Commissioner of the Regional Government.

Triaxial accelerometers were rigidly attached to the head, T1, T8, L2 and the pelvis. ARS were added to the head and T1. Linear acceleration was measured at the location of the sternum body. Photo targets were used to identify relevant landmarks, including the location of the external auditory meatus bilaterally. These photo targets were used to track the displacement of the center of gravity of the head in the sagittal plane.

**RESULTS**

**Upper shoulder belt force**

Figure 1 shows the time history plot of the belt tension measured at the upper shoulder belt location in the THOR sled tests. Red solid lines correspond to the SB seatbelt while blue solid lines are the forces measured in the PT+FL belt tests. Apart from the greater pretensioner force of the SB seatbelt, two out of the three tests with the SB seatbelt resulted in a higher peak force than in the case of the PT+FL seatbelt (PT+FL: 5465.7 ± 212.7 N; SB: 6124.7 ± 706.6 N). Figure 1 also shows that the SB seatbelt induced a bimodal force curve on the ATD with the first and higher peak ocurring at around 100 ms followed by a smaller peak at approximately 135 ms. The second maximum observed when the SB seatbelt was used contributed to the longer interaction between the occupant and the restraint: while the magnitudes of the force-time traces of the PT+FL seat belt are almost negligible at t=120 ms, the curves corresponding to the SB seatbelt indicate that the occupant was still being restrained by the seatbelt up to t=150 ms.

The time traces in Figure 2 show the time history of the upper shoulder belt forces in the PMHS tests. The peak force sustained by the occupant when the SB seat belt was used was higher than in the case of the PT+FL seat belt (6109.7 N vs. 4133.51 N). the longer interaction of the occupant with the restraint that was observed with THOR is also present in the PMHS tests, although there is no secondary peak in this case.

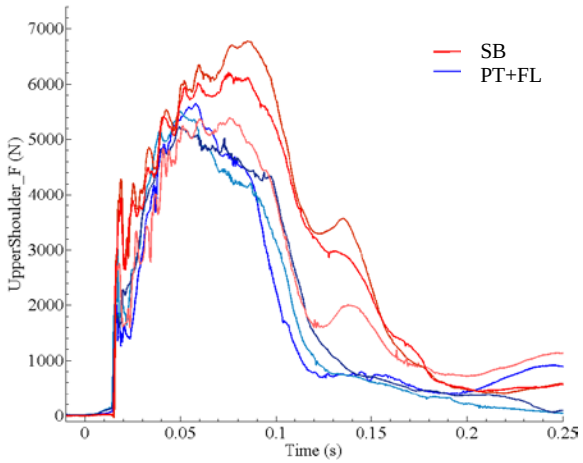


***Figure 1 Time history of the upper shoulder belt force measured in the dummy tests***

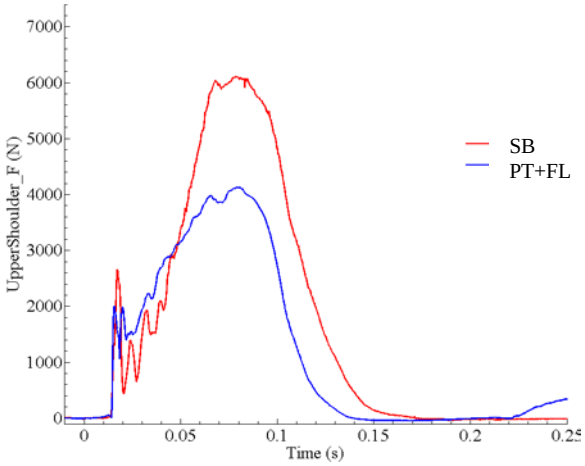


***Figure 2. Time history of the upper shoulder belt force estimated in the PMHS tests.***

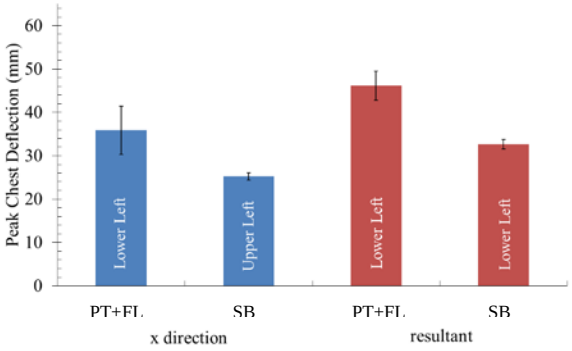


***Figure 3 THOR peak chest deflection in mm in the local x-direction (blue bars) and resultant (red bars) as measured by the IRTRACCs, with error bars corresponding to the standard deviation. Labels within the bars indicate the IRTRACC sensor recording the peak deflection.***

**THOR chest deflection**

The peak chest deflection in the local x-direction (initially aligned with the motion of the sled, but moving with the ATD torso) was measured at the lower left IRTRACC when the PT+FL seatbelt was used while it ocurred at the location of the upper left IRTRACC with the SB due to the higher forces applied to the shoulder of the occupant. In addition, the peak deflection was greater with the PT+FL seatbelt (35.9 ± 5.6 mm vs. 25.2 ± 0.8 mm). When the three components of the deflection were combined into the calculation of the peak resultant deflection, still the PT+FL seatbelt resulted in a greater magnitude (46.2 ± 3.4 mm vs. 32.7 ± 1.1 mm). However, the resultant peak deflection was measured at the lower left chest location regardless of the restraint used.

**Head displacement in the sagittal plane**

The displacement in the sagittal plane of the center of gravity of the head of THOR and the PMHS is shown in Figure 4 and Figure 5. Blue solid lines correspond to the PT+FL seatbelt and red solid lines to the SB seatbelt.

Peak forward displacements of the head center of gravity of THOR were not significantly different for the two restraints under analysis (PT+FL: 390.7 ± 11.1 mm; SB: 406.4 ± 6.7 mm). Figure 4 illustrates that the nature of the trajectory of the head center of gravity was similar under the action of the two different restraints. Other than slight differences in magnitude, it is not possible to identify different trends or behaviors. Regardless of the restraint, the head center of gravity moved straight forward and slightly downwards up to t=50 ms and then it started to describe a curvilinear trajectory.

As the statures of the two PMHS were different, trajectories were length-scaled to those of a 50$^{th}$ male percentile (nominally, 175 cm). Figure 5 shows the comparison of the scaled trajectories followed by the center of gravity of the PMHS head depending on the seatbelt used. The use of the SB resulted in a greater forward excursion (306.1 mm vs. 188.8 mm). The maximum vertical excursion of the two seatbelts were not substantially different. The shape of the trajectories differed importantly. While the use of the SB seatbelt resulted into an initial forward displacement of the center of gravity of the head that occurred parallel to the local X axis for about 70 ms, the use of the PT+FL seatbelt caused the PMHS head to describe a curvilinear trajectory from the first instants of the deceleration. The analysis of the high-speed video images indicated that while the SB seatbelt allowed the spine of the dummy to pitch forward and rotate, the PT+FL seatbelt impeded the flexion of the PMHS spine resulting into the curvilinear motion of the head center of gravity in which the lower neck acted as fulcrum of the rotation. There are two reasons that contribute to the differences observed in the kinematics of the spine of the PMHS. The first one is that the higher lap belt forces of the SB seatbelt facilitated that the pelvis of the PMHS almost did not move forward during the impact, while the pelvis of the PMHS that was restrained with the PT+FL slid during the deceleration over the flat surface of the seat. The forward pelvic motion caused the occupant to adopt a slouched position and prevented the torso from pitching forward as it would have been desirable. The second reason is that the analyses of the lower shoulder belt forces show that even if the peak force is much higher when the SB seatbelt was used (4729.0 N vs. 3461. 6 N, see Table 2), the PT+FL lower shoulder belt force was higher up to t=70 ms and therefore the torso of the occupant was subjected to a higher force that could have impeded the rotation during the first stages of the deceleration. In fact it is around t=70 ms that the torso of the PMHS restrained with the SB belt stopped its rotation and the head started to describe a curvilinear trajectory.

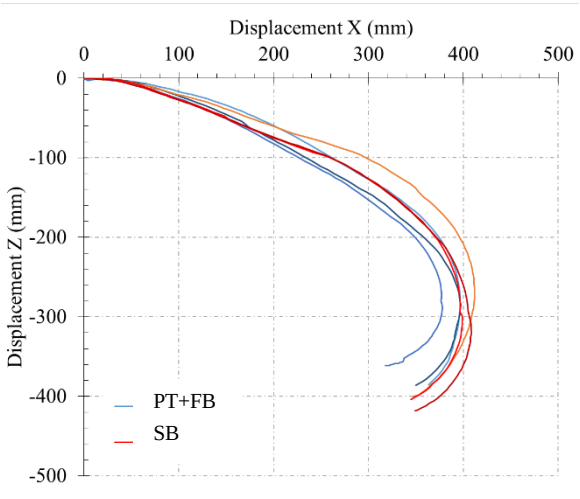


***Figure 4 Displacement of the center of gravity of THOR head in the sagittal plane.***

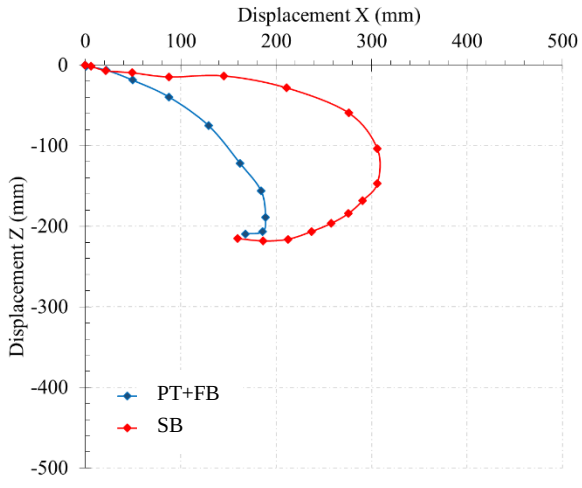


***Figure 5 Displacement of the center of gravity of the PMHS head in the sagittal plane. Trajectories are scaled to represent a 50$^{th}$ male percentile.***

## DISCUSSION

The concept design of the split buckle restraint system (SB) intended to increase the loading on anatomical parts that are potentially more likely to bear higher loads (i.e. clavicle, pelvis) so that the amount of restraint loading on the chest could be lowered without modifying significantly the forward displacement of the head. The assessment of the system was done using two different occupant surrogates: the THOR dummy and PMHS in sled frontal impacts with a delta-v = 35 km/h (nominally). A pretensioned, force limiting seatbelt (PT+FL) was

used as reference for the assessment. The data generated in these tests can be used to benchmark numerical models, so that parametric studies can be done to find the optimal geometry of the split buckle seat belt [20].

The tests with the THOR dummy showed that the use of the SB belt system resulted into slightly higher upper shoulder belt forces, considerably higher lower shoulder forces and higher bilateral lap belt forces as well. However, resultant chest deflection and local x-axis chest deflection as measured by the IRTRACCs of the dummy were reduced for all measurement locations with the exception of the upper left IRTRACC, in which the magnitudes were not significantly different. Comparable results regarding belt forces were observed also in the PMHS tests, confirming the predictions given by THOR. Despite the associated higher SB shoulder belt, the duration of the engagement between belt and occupant was longer than in the PT+FL case, which resulted in smaller sternal deceleration of the occupant (see Table 2).

As for the displacement of the head in the sagittal plane, Figure 4 illustrates that THOR did not capture significant differences in nature between the two belt systems. In addition, the peak forward displacement of the center of gravity was similar regardless of the belt used (PT+FL: 390.7±11.1 mm vs. SB: 406.4±6.7 mm). The tests with the PMHS showed very different results in this case. While the SB system resulted in a trajectory in which the head moved forward first parallel to the local X axis and then underwent a curvilinear translation, when the PT+FL system was used, there was almost no forward motion of the torso of the PMHS resulting into a curvilinear translation of the head from the beginning of the deceleration. Consequently, the magnitude of the peak forward displacement of the head was smaller in this case (PT+FL: 188.8 mm vs. SB: 306.1 mm). However, the analysis of the high-speed video images showed that while the SB lap belt prevented the forward displacement of the PMHS pelvis, the PT+FL belt allowed the pelvis of the occupant to move forward. The forward motion of the pelvis associated to the lack of torso pitch are indicative of poor occupant kinematics that could result in submarining. Of course, the flat design of the seat is playing an important role in the deficient control of the motion of the pelvis as indicated in previous work using the same test fixture [21]. These differences in the kinematics of the pelvis and the torso were not observed in the sled tests with the THOR dummy. Even if the pelvis of the dummy moves forward during the initial instants of the deceleration until it is arrested by the lap belt, the torso of the dummy rotates up to the moment of maximum shoulder belt tension in which the head starts to undergo flexion. Regardless of the seatbelt used, the analysis of the kinematics of THOR does not indicate that submarining occurred in the tests.

The test fixture, except for the restraint type used, is a replica of that used in previous studies aiming to assess the biofidelity of THOR and to develop a new chest injury criterion for this ATD [22]. In the present study, the knee bolster used in [22] was removed. The only other set of PMHS and dummy tests that were run with this fixture without knee bolster compared the kinematics of the Hybrid with the kinematics of PMHS in frontal impacts conducted at 9 km/h [23]. In this case, non-pretensioned, non force-limiting seat belts were used. Recorded peak upper shoulder belt forces were in the range between 1000 kN and 1250 kN, and peak forward head displacement of the three tested PMHS ranged between 280 and 310 mm. Two remarks are relevant from this study. First, the nature of the motion of the head was similar to that observed in the present study for the SB seat belt: an initial trajectory parallel to the sled X-axis followed by a curvilinear trajectory once the upper shoulder force peaked. Secondly, while THOR predicted greater forward head excursion compared to the PMHS, the Hybrid III (178±2 mm) fell short to predict the displacement of the PMHS heads.

The magnitude of the upper and lower neck reactions (forces and moments) in THOR were similar regardless of the seat belt system used in the test. Measured values were considerably smaller than those proposed in existing IARV (Mx=143 Nm; My=190 Nm; Mz=96 Nm; Fz=4 kN; Fx=Fy=3.1 kN) [24]. Neck reaction forces were not calculated for the PMHS, but the comparison of the values measured for the acceleration and angular rate of the head indicated that the SB belt induced higher linear acceleration than the PT+FL seat belt, and consequently the upper neck loads would have been slightly greater.

**Table 2.**
**Peak value comparison of selected parameters between the PT+FL and the SB belt.**

| | PT+FL | | SB | |
|---|---|---|---|---|
| | **THOR test*** | **PMHS test** | **THOR test*** | **PMHS test** |
| Head acceleration** (g) | | | | |
| x | -19.8±2.8 | 10.4 | -22.7±1.4 | 28.5 |
| y | 3.9±1.0 | 29.8 | 2.3±0.5 | -58.1 |
| z | 32.9±2.0 | 33.5 | 38.4±7.0 | 50.7 |
| Head angular rate (deg/s) | | | | |
| x | -767.1±22.8 | -2170.0 | -635.4±99.5 | 2078.1 |
| y | -1798.9±92.0 | 579.8 | -2079.6±149.8 | 419.8 |
| z | -681.5±18.1 | 300.4 | -639.5±110.7 | 1001.0 |
| Upper neck | | | | |
| Fx (kN) | 1.2±0.4 | - | 1.1±0.0 | - |
| Fy (kN) | 0.2±0.0 | - | 0.2±0.1 | - |
| Fz (kN) | 1.4±0.1 | - | 1.8±0.1 | - |
| Mx (Nm) | -21.7±3.1 | - | -19.0±96.8 | - |
| My (Nm) | 22.0±0.2 | - | 21.6±2.1 | - |
| Mz (Nm) | -5.4±0.6 | - | 2.9±1.3 | - |
| Lower neck | | | | |
| Fx (kN) | 0.6±0.2 | - | 0.5±0.1 | - |
| Fy (kN) | 0.5±0.3 | - | 0.2±0.1 | - |
| Fz (kN) | -1.2±0.2 | - | -1.6±0.1 | - |
| Mx (Nm) | 55.0±8.0 | - | 58.8±5.2 | - |
| My (Nm) | 23.8±8.3 | - | 25.5±0.8 | - |
| Mz (Nm) | -18.4±4.1 | - | -19.1±4.3 | - |
| Chest acceleration (g) | - | -143.0 | - | -106.1 |
| Pelvis acceleration (g) | | | | |
| x | -11.3±0.6 | -38.7 | -15.5±0.9 | -59.4 |
| y | -9.3±4.5 | -36.4 | -8.6±4.1 | 27.7 |
| z | -18.3±1.7 | -25.7 | -19.0±2.1 | -22.6 |
| Head maximum forward displacement (mm) | 390.7 ± 11.1 | 188.8 | 406.4 ± 6.7 | 306.1 |
| IRTRACC (Resultant, mm) | | | | |
| Upper Left | 31.8±1.5 | - | 32.1±0.8 | - |
| Lower Left | 46.2±3.4 | - | 32.4±1.0 | - |
| Upper Right | 31.7±2.9 | - | 31.8±1.4 | - |
| Lower Right | 26.6±2.9 | - | 21.4±1.0 | - |
| IRTRACC (x direction, mm) | | | | |
| Upper Left | 24.2±0.5 | - | 25.1±0.9 | - |
| Lower Left | 35.9±5.6 | - | 24.5±1.8 | - |
| Upper Right | 17.0±14.3 | - | 8.0±0.9 | - |
| Lower Right | 18.1±8.0 | - | 12.3±0.2 | - |
| Upper shoulder belt force (N) | 5465.7 ± 212.7 | 4133.5 | 6124.7 ± 706.6 | 6109.7 |
| Lower shoulder belt force (N) | 3998.5±156.0 | 3461.6 | 5055.5±575.7 | 4729.0 |
| Right lap belt force (N) | 2001.8±20.6 | 1634.5 | 3133.3±48.0 | 2053.5 |
| Left lap belt force (N) | 2059.3±542.6 | 3324.7 | 2971.9±22.6 | 7367.7 |

* Values for THOR shown as average ± standard deviation.

** Magnitude measured with respect to a local coordinate system with origin in the head attachment plate, not transferred to the head center of gravity.

**Limitations**

Even if the test fixture has been utilized before in the assessment of the biofidelity of ATD and in the development of thoracic ATD injury criteria, it is questionable its utility in the assessment of restraint systems. The simple geometry and the completely rigid structure of the seat facilitated the forward motion of the pelvis of the PMHS restrained with the PT+FL and the subsequent differences in torso pitch with respect to the other seatbelt solution. A regular production seat would have reduced the forward motion of the pelvis and contributed to increase the forward rotation of the torso.

Some channels of the external data acquisition system malfunctioned during the THOR tests. In particular, the upper shoulder belt load cell did not measure correctly the tension of the belt. To overcome this issue, a methodology was developed so that the magnitude of the belt tension at the upper shoulder location could be estimated using the measurement from the lower shoulder belt. The methodology is explained within the Appendix, and it was built using previously sled tests ran with both restraint systems. The correlation factor of the relationship found between the upper and lower belt tension magnitudes were $R^2$= 0.98 (PT+FL) and $R^2$= 0.99 (SB).

One additional limitation is the magnitude variability observed in the deceleration pulse between the two PMHS experiments that reached almost 4g at its peak difference. Although this difference would have hindered a detailed quantitative comparison between the performance of the two systems, the differences in the nature of the kinematics suggest that these differences were not related to just a change in the magnitude of the mechanical insult but to the way in which the restraints interacted with the PMHS. Interestingly, these differences were not observed when the surrogate chosen was THOR.

## CONCLUSIONS

The present study compares the kinematics and dynamics of the THOR dummy and two PMHS in frontal impacts at 35 km/h using two different seat belts. One belt was a pretensioned force-limiting seatbelt that was used to benchmark a new concept consisting of two separate shoulder and lap bands, equipped with pretensioners at the shoulder belt retractor and at both lap belt anchorages. The aim of the SB model was to increase the load on the clavicle and pelvis to unload the chest region, without increasing significantly the forward displacement of the head comparing to the benchmark. The sled tests performed with THOR confirmed the intended performance of the concept belt and the chest deflection measured by the IRTRACC was substantially lower in comparison with the PT+FL seatbelt. The two PMHS exhibited very different kinematics depending on the seatbelt used. While the PT+FL seatbelt allowed the pelvis to move forward, reducing torso pitch and therefore inducing a curvilinear motion of the head, the SB allowed substantial torso pitch resulting on increased forward excursion of the head that moved initially in a rectilinear fashion undergoing a curvilinear trajectory only once the torso motion was completely arrested. Given the limited number of PMHS tests, it is not possible to conclude if the particularities of the individual PMHS were the cause of the differences or if THOR failed to capture the kinematics of an actual subject under the action of these seat belts.

## ACKNOWLEDGEMENTS

Autoliv Research collaborated in this study providing access to the THOR dummy and the restraint systems. It was partially funded by the Instituto Aragones de Fomento of Gobierno de Aragon via the "Collaborative agreement to foster research on impact biomechanics", signed on Feb 11th, 2015. The PMHS tests were performed within the BIO-ADVANCE project (Marie Curie Actions, FP7/2007-2013, REA grant agreement no. 299298). More information about this project and its goals can be found in [19]. The analyses presented here were not generated during the project and do not represent necessarily the position of the researchers involved in BIO-ADVANCE. This study shows solely the interpretation of the authors and is not necessarily the view of Autoliv Research or the Instituto Aragones de Fomento.

## REFERENCES

[1] European Commission. Commission Communication - The demographic future of Europe – From challenge to opportunity (2006)

[2] EuroStat. Fertility rates - Statistics explained (2013): http://epp.eurostat.ec.europa.eu/statistics_explained/index.php/Fertility_statistics#Publications. Last accessed: 01/02/2014.
[3] United Nations, Department of Economic and Social Affairs, Population Division (2013). World Population Ageing 2013. ST/ESA/SER.A/348
[4] European Road Safety Observatory (ERSO) Website, Factsheet the Elderly (> 64 years) Traffic Safety Basic Facts 2012, DACOTA Project.
[5] Kent R, Trowbridge M, Lopez-Valdes FJ et al. How many people are injured and killed as a result of aging? Frailty, fragility, and the elderly risk-exposure tradeoff assessed via a risk saturation model. Annals of Advances in Automotive Medicine, 2009. Vol. 53, 40-50.
[6] Scarboro M. Real World Older Occupant Injury. SAE Government / Industry meeting. January 2014. Washington DC, USA. Available at : http://www.nhtsa.gov/Research/Public+Meetings/SAE+2014+Government+Industry+Meeting.
[7] Kent R, Crandall JR, Bolton J, Prasad P, Nusholtz G, Mertz H. The influence of superficial soft tissues and restraint conditions on thoracic skeletal injury prediction. Stapp Car Crash J. 2001;45:183–204.
[8] Walz M. NCAP test improvements with pretensioners and load limiters. Traffic Inj Prev. 2004;5:18–25.
[9] Forman JL, Michaelson J, Kent R, Kuppa A, Bostrom O. Occupant restraint in the rear seat: ATD responses to standard and pre-tensioning, force-limiting belt restraints. AnnAdvAutomotMed. 2008;52:141–154.
[10] Forman JL, Lopez-Valdes F, Lessley D, et al. Rear seat occupant safety: an investigation of a progressive force-limiting, pretensioning 3-point belt system using adult PMHS in frontal sled tests. Stapp Car Crash J. 2009;53:49–74.
[11] Forman JL, Lopez-Valdes F, Dennis N, Kent R, Tanji H, Higuchi K. An inflatable belt system in the rear seat occupant environment: investigating feasibility and benefit in frontal impact sled tests with a 50th percentile male ATD. Ann Adv Automot Med. 2010;54:111–126.
[12] Kent R, Lopez-Valdes FJ, Dennis NJ, et al. Assessment of a three-point restraint system with a pre-tensioned lap belt and an inflatable, force limited shoulder belt. Stapp Car Crash J. 2011;55:141–159.
[13] Sundararajan S,Rouhana SW, Board D, et al. Biomechanical assessment of a rear-seat inflatable seatbelt in frontal impacts. Stapp Car Crash J. 2011;55:161–197.
[14] F. J. Lopez-Valdes, O. Juste, B. Pipkorn, I. Garcia-Muñoz, C. Sunnevång, M. Dahlgren & J. J. Alba (2014) A Comparison of the Performance of Two Advanced Restraint Systems in Frontal Impacts, Traffic Injury Prevention, 15:sup1, S119-S125, DOI: 10.1080/15389588.2014.936410
[15] Lopez-Valdes FJ, Lau A, Lamp J, et al. Analysis of spinal motion and loads during frontal impacts. Comparison between PMHS and ATD. Ann Adv Automot Med. 2010;54:61–78.
[16] Shaw G, Parent D, Purtsezov S, et al. Impact response of restrained PMHS in frontal sled tests: skeletal deformation patterns under seat belt loading. Stapp Car Crash J. 2009;53:1–48.
[17] Hynd D, Carroll J, Davidsson J, Vezin P. Biofidelity Requirements for the THORAX Project. THORAX D2.1 European Commission DG RTD 7th Framework Program.
[18] Lemmen P, Been B, Carroll J, et al. An advanced thorax–shoulder design for the THOR dummy. In: Proceedings of the 23rd ESV Conference, Seoul, Korea, 2013.
[19] BIO-ADVANCE (Advancing traffic safety through the investigation of human tolerance to impact). Marie Curie Actions. Final Report. Project No. 299298. 2014. European Commission.
[20] Pipkorn B, Lopez-Valdes FJ, Lundgren C, Brase D, Sunnevang C. Advanced seat belt system for reduced chest deflection. Paper No. 15-0371. 24th International Technical Conference on the Enhanced Safety of Vehicles (ESV). Gothenburg, Sweden, June 8-11, 2015
[21] Lopez-Valdes FJ, Juste Lorente, O, Pipkorn B, Garcia I, Sunnevang C, Dahlgren M, Alba J. (2014) A comparison of the performance of two advanced restraint systems in frontal impacts. Traffic Injury Prevention. Volume 15, Supplement 1, 2014: S119-S125.
[22] Shaw G, Parent D, Purtsezov S, Lessley D, Crandall J, Kent R, Guillemot H, Ridella S, Takhounts E, Martin P. Impact Response of Restrained PMHS in Frontal Sled Tests: Skeletal Deformation Patterns Under Seat Belt Loading. Stapp Car Crash Journal.Vol. 53, pp 1-48, 2009.
[23] Lopez-Valdes FJ, Lau A, Lamp J, Riley P, Lessley DJ, Damon A, Kindig M, Kent R, Balasubramanian S, Seacrist T, Maltese M, Arbogast K, Higuchi K, Tanji S (2010). Analysis of spinal motion during frontal impacts. Comparison between PMHS and ATD. Ann Adv Automot Med. 2010;54:61-78.
[24] Mertz HJ, Irwin AL, Prasad P. Biomechanical and scaling bases for frontal and side impact injury assessment reference values. Stapp Car Crash Journal, Vol. 47 (October 2003), pp. 155-188.

## APPENDIX

### Sled deceleration

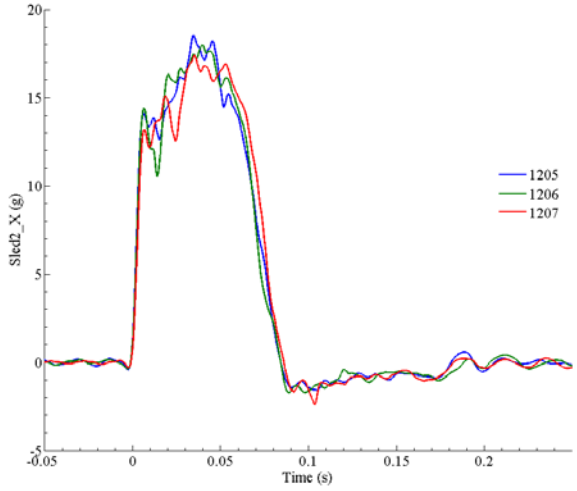


*Figure A1. Time history of the deceleration of the sled. THOR tests.*

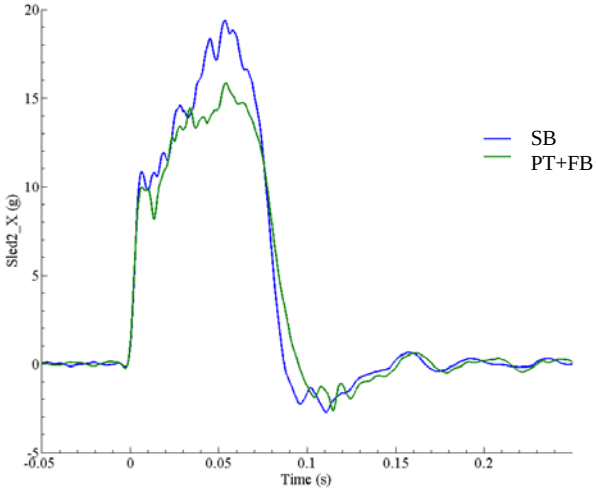


*Figure A2. Time history of the deceleration of the sled. PMHS test.*

### Estimation of upper shoulder belt forces (THOR tests)

The channel associated to the measurement of the tension at the upper shoulder belt location failed during the THOR tests. The input voltage fluctuated during the tests and, consequently, the measure of belt force was erroneous. To provide a reasoned estimation of the tension of the belt at this location, previous sled tests performed using the same deceleration pulse and the THOR dummy were used to find a correlation between the tension of the shoulder belt at the upper (close to the clavicle) and lower locations (close to the abdomen). It was found that a linear relationship could be established between these two measurements and therefore, the upper shoulder force could be estimated based on the measurement obtained at the lower location. The correlation factors obtained in the estimation of the upper shoulder belt force were $R^2$= 0.98 (FL+PT belt) and $R^2$=0.99 (SB belt) (see Figures A3 and A4).

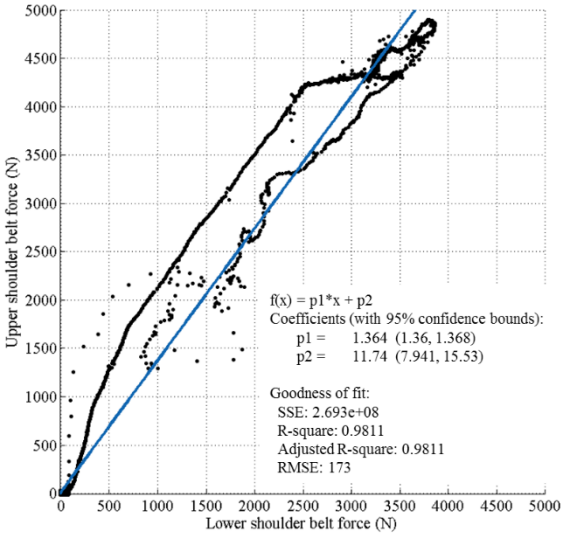


*Figure A3. Linear relationship (blue solid line) existing between the shoulder belt forces measured at the upper and lower locations. FL+PT belt.*

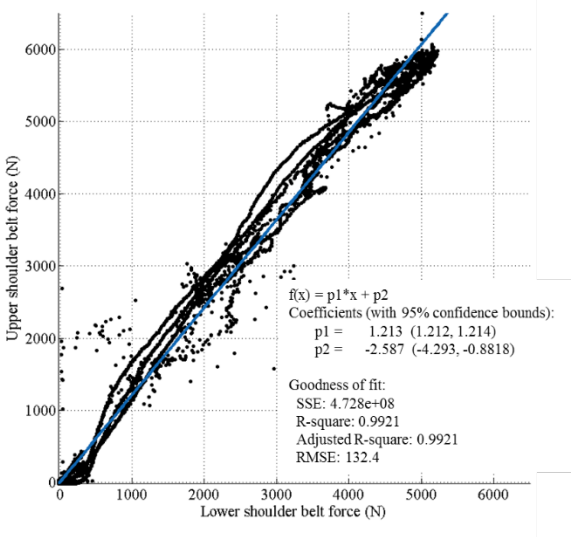


*Figure A4. Linear relationship (blue solid line) existing between the shoulder belt forces measured at the upper and lower locations. SB belt.*